Algorithm for the charge-coupled-device scanning actinic flux spectroradiometer ozone retrieval in support of the Aura satellite validation

Irina Petropavlovskikh,[1] Richard Shetter,[2] Samuel Hall,[3] Kirk Ullmann,[3] and Pawan K. Bhartia[4]

[1] Cooperative Institute for Research in Environmental Sciences, University of Colorado, Boulder, CO 80305, USA
irina.petro@noaa.gov

[2]National Suborbital Education and Research Center, University of North Dakota, Grand Forks, ND, USA
r.shetter@nserc.und.edu,

[3] Atmospheric Chemistry Division, ESSL, NCAR, Boulder, Colorado, USA
halls@ucar.edu, ullmannk@ucar.edu

[4] Atmospheric Chemistry and Dynamics Branch, NASA Goddard Space Flight Center, Greenbelt, Maryland, USA
Pawan.K.Bhartia@nasa.gov

Abstract. Stratospheric ozone column data was acquired during four recent aircraft-based validation missions for the Aura satellite flown in years 2004-2006. The data was retrieved by the spectrally-resolved actinic flux measurements of the charge-coupled-device scanning actinic flux spectroradiometer (CAFS) instrument carried on board the NASA WB-57 and DC-8 aircrafts. Each dataset contains information on temporal and spatial variability in the stratospheric ozone column. Analyses of the CAFS datasets provide guidance for assimilation of data from individual satellite orbits into the global maps of stratospheric ozone. Moreover, the 10-second samplings of the CAFS data supply information on spatial variability of stratospheric ozone column across the footprint of a satellite measurement. The CAFS data is available as a function of altitude and geo location of the aircraft. This paper describes the algorithm for the retrieval of an ozone column above the aircraft level, along with validation of the CAFS retrieved ozone product. A discussion of the retrieval uncertainty is provided with emphasis on the algorithm's assumptions and instrumental uncertainties. Sensitivity of the ozone retrieval to fundamental atmospheric parameters is discussed in detail, and the range of uncertainties is estimated under a variety of observational conditions. The characteristic model uncertainty of the CAFS partial ozone column retrieval is better than 3 %, whereas the CAFS measurement precision contributes less than 1 % to the retrieval uncertainty.

Keywords: remote sensing, algorithm, radiative transfer, ozone

1 INTRODUCTION

One of the primary objectives of the EOS-Aura Mission is to determine if the ozone layer is recovering as predicted by atmospheric models [1]. The four instruments on the Aura platform (High Resolution Dynamics Limb Sounder (HIRDLS), Tropospheric Emission Spectrometer (TES), Microwave Limb Sounder (MLS) and Ozone Monitoring Instrument (OMI)) take global ozone measurements at different spatial and temporal resolution. An important part of the overall Aura mission is to provide validation of the satellite's measurements. Therefore, ground, aircraft, and balloon based campaigns have been implemented. The goal of recurring Aura Validation Experiments (AVE) is to provide

Received 21 Mar 2007; accepted 12 Sep 2007; published 5 Oct 2007 [CCC: 19313195/2007/$25.00]

correlative measurements from the National Aeronautic and Space Administration (NASA) aircraft at a variety of locations to cover the geographical and altitude range of the Aura products. Moreover, airborne measurements are done at high spatial resolution and can detect small-scale spatial variability in the atmosphere across the satellite footprint. Therefore, an impact of atmospheric variability on satellite retrieval products can be assessed from the airborne information. As satellites use traditional methods of validation against the well-established ground-based measurement networks, the aircraft measurements are designed to fly to any geographical location. The aircraft based missions can also provide atmospheric "slicing" by spiraling to lower/higher altitudes to scan for vertical distribution of atmospheric species within the satellite's footprint.

This paper describes the newly developed ozone retrieval algorithm for the new solar radiation measurement instrumentation deployed on the NASA WB-57 and DC-8 platforms (http://www.nasa.gov/centers/dryden/research/AirSci/index.html). The spectrally resolved UV actinic flux obtained in flight is used in conjunction with radiative transfer calculations to obtain ozone column abundances above the aircraft altitude. The CCD (Charge Coupled Device) Scanning Actinic Flux Spectroradiometer (CAFS, Hall et. al. in preparation) collects up and down welling actinic flux data. An extensive dataset of ozone column abundances above the airborne platform have been collected during four AVE missions in 2004, 2005 and 2006. The dataset is available for the Aura ozone validation activities through Aura Validation Data Center at NASA, Goddard Space Flight Center (http://avdc.gsfc.nasa.gov).

We also provide assessment of retrieval uncertainties associated with measurement accuracy, direct model assumptions, and other factors. Finally, we introduce results of validation against well characterized systems. Validation of Aura satellite data against CAFS derived partial ozone column will be described in a separate paper. The next section provides basic information about the CAFS instrument that is necessary for the discussion of instrumental uncertainties. The detailed description of the instrument will be given in a paper by S. Hall et al (in preparation).

2 INSTRUMENTS AND DATA

2.1 CCD Actinic Flux Spectroradiometer

New solid state, CCD based spectroradiometer instruments have been developed in the Atmospheric Radiation Investigations and Measurements (ARIM) laboratory under the National Center for Atmospheric Research (NCAR) for deployment on the NASA WB-57 and other platforms (Figure 1). The systems are based on the 2π steradian hemispherical zenith and nadir viewing optical collectors connected with UV fiber optic bundles to small, lightweight, monolithic monochromators equipped with cooled CCD detectors, and small, lightweight, low-power PC-104+ computers for autonomous instrument control and data acquisition.

The system employs a Zeiss MCS (Multi Channel Spectrometer) monolithic monochromator equipped with a Hamamatsu S 7301-906 windowless back-thinned blue enhanced 534 pixel cooled CCD detector. The combination of the monochromator, slit size and CCD provides a wavelength range of 280-680 nm with an effective ~1.8 nm Full Width at Half Maximum (FWHM) resolution with a 20 micron entrance slit (see section 2.4 for further information on the CAFS slit functions). The CCD temperature is controlled at –1.0 degrees C by a piezoelectric cooler and control electronics. The system exhibits excellent sensitivity from the ultraviolet into the visible, which allows rapid full spectral acquisition times from 100 ms.

The CCD monochromator assembly is contained in a sealed instrument box to prevent moisture condensation on the CCD elements and maintain temperature control. An entire spectroradiometer system weighs approximately 23 kg and is designed to be mounted in the

radiation boat on the top of the fuselage and in the bottom transition area of the WB-57. The spectrometer and data systems require <15 A of 28 VDC per instrument.

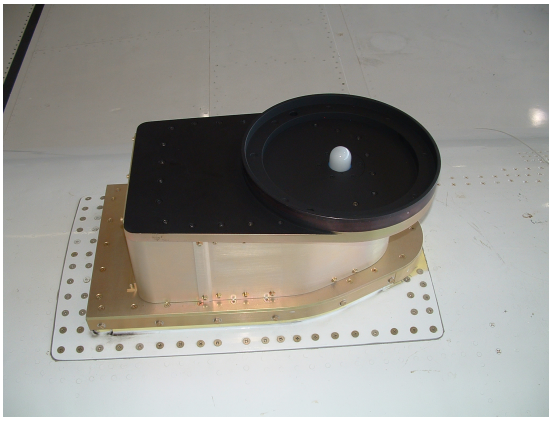

Fig. 1. In-flight configuration of CAFS instrument is shown mounted at upper equipment bay on the NASAWB-57 aircraft. Picture was taken during the AVE 2005 campaign in Houston, TX.

2.2 Instrument Development and Deployment

The CAFS instrument has been flown in four missions. The CAFS instrument was initially deployed on the WB-57 in October 2004 for the first AVE campaign based off Houston, TX (AVE04). During AVE04 experiment a total of eight science flights were conducted to support AURA validation campaign. The following AVE mission, P-AVE05, deployed the DC-8 aircraft that was based in Pease, Massachusetts in January and February of 2005. During P-AVE05 campaign a total of 8 science flights were flown over a vast range of geophysical conditions including fields with large ozone variability over the Northern high latitudes. The 2005 AVE mission out of Houston (8 science flights) and 2006 AVE mission out of Costa Rica, CR-AVE, (14 science flights) deployed WB-57 aircraft.

Prior to AVE Houston 2005, the temperature control systems were redesigned to provide more consistent control of the temperature at altitude. The redesign included additional thermistors, heaters, PID controllers, circulating fans and a new insulation design for the spectrometer housing. The data acquisition computer enclosure was encased in foam insulation and heaters and click thermostats were added to maintain temperature and avoid moisture condensation on aircraft descent.

The data algorithm development team established that near horizon radiation was degrading the accuracy of the retrieval algorithm. Therefore, after the PAVE05 mission, the artificial horizon in the CAFS down-welling instrument sky-views was raised to about 10 degrees above the aircraft platform. The modifications were applied to the existing optical system and are completely reversible. The detailed angular response of the system with the modified horizon was determined and provided as a model input for the ozone column algorithm. The optical collector design was also modified to insure the sealing of the enclosure. The data acquisition software also was improved to overcome errors introduced by static electricity discharge along the aircraft frame encountered during early deployments. Extra housekeeping parameters were added to improve monitoring of in-flight temperature stability. Redundant flash drive data storage was added to allow immediate data retrieval on landing, without having to apply power to the systems.

The NCAR/ARIM group continued to deploy revised CAFS instruments on the WB-57 for the Costa Rica AVE mission in January and February 2006. The instrument was prepared,

calibrated, integrated, and test flown on the WB-57 at Johnson Space Center in Houston, TX. Instrument calibrations were performed in the field to track the wavelength registration and spectral calibration during the mission. Improvements in the calibration mount allowed one calibration system to service both upper and lower CAFS systems and improved the consistency of the calibrations. The instrument response has shown a slight dependence on the CCD temperature. In an attempt to eliminate this shift, external cooling was employed for ground calibrations to better represent in flight thermal conditions. Since the CAFS mounting locations were outside of the pallet bay, this allowed the CAFS instruments to contribute to both the remote and in-situ portions of the CR-AVE mission. Details of the instrument's design and results of final calibrations performed in the laboratory at NCAR will be described in the separate paper (S. Hall et al, in preparation).

2.3 Other instruments and data

Ozone-sonde data from stations across the USA, Canada and Costa-Rica (including the station at San Cristobal, Ecuador) have been archived at NASA's mission-dedicated data archive centre (http://avdc.gsfc.nasa.gov/). The special ozone-sondes were flown from ground-based stations to support AVE missions during 2004, 2005 and 2006. The accuracy of the sonde profile depends on the type of the sensor and the chemical solution used in the measurements [2][3][4]. The accuracy of the Electrochemical Concentration Cell (ECC) ozone sonde profiles is estimated to be better than 5 % in the stratosphere and troposphere. Ozone information above the balloon's burst level is commonly estimated from the ozone climatology based on the Solar Backscatter UltraViolet Instrument (SBUV) ozone profile data [5], or is traditionally normalized to the total ozone column from the Dobson or Brewer measurements if the latter two are available at the station. The accuracy of the integrated sonde profile is typically better than 10 %.

The Dobson spectrophotometer network has been extensively operated since 1957 and successfully generated a long-term total ozone column time-series. The ozone column is generally derived from the direct-sun measurements taken at nominal wavelengths in the UV Solar spectrum [6] [7]. However, it can be also deduced from zenith-sky radiance measurements in case of the low elevation of the sun or whenever the sun is obscured by clouds. The worldwide network of Dobson instruments is well calibrated and has a traceable history of intercomparisons and calibrations, while the world standard instrument is maintained at the National Oceanographic and Atmospheric Administration (NOAA) in Boulder, CO, USA. The Dobson total ozone column data has been successfully used in the past to provide rigorous validation for a variety of satellites such as TOMS (Total Ozone Mapping Spectrometer), SBUV, etc. [8] [9].

The Microtops instruments are filter-based photometers that derive ozone column from direct-sun measurements in several UV spectral channels. The instrument uses GPS information to set the time, longitude and latitude of the location for air-mass calculations. The instrument is very small and is easily transported to remote areas where no other traditional ozone measuring techniques are available. One instrument was used to take measurements during CR-AVE 2006 campaign (owned by the Atmospheric Chemistry and Dynamics Branch of NASA/Goddard). Although Microtops instruments are regularly calibrated against the Brewer instrument at NASA/Goddard (private communications with G. Labow, NASA/Goddard), several days of coincident measurements were used to perform comparisons against the world standard Dobson instrument in Boulder, CO (NOAA, Environmental Systems Research Labs). The results of the comparisons suggest that the accuracy of the tested Microtops instrument is within 2 % of the direct-sun standard Dobson measurements. However, these results are instrument specific and may be not be true for any other Microtops instrument.

Several coincidental and complimentary ozone measurements were taken during the CR-AVE campaign in Costa Rica in January and February 2006. The Microtops measurements were collected on the ground at the airport of San Jose, Costa Rica, and were performed every hour whenever the sun was not blocked by the clouds. The ozone sounding launch was timed to coincide with the WB-57 flight over the University of Costa Rica in San Jose. The CAFS measurements were carried out on board of the WB-57. The detailed discussion of the cross-referenced dataset will be given in Section 6.

2.4 Measurement uncertainty, precision and accuracy

The accuracy of the CAFS actinic flux measurements is related to the uncertainty in the calibrated flux of the National Institute of Standards and Technology (NIST) traceable irradiance standards, the 2 π steradian light collection efficiency, and other instrumental uncertainties in wavelength registration and band-pass. The overall CAFS uncertainty is largely a function of the calibration lamp uncertainty that is estimated at 5% in the UV-B and 3% in the UV-A (see Table 1). The precision of the measurements is a function of the instrument stability. The spectrometer bodies are ceramic and the entrance optics and CCD detectors are permanently attached to the spectrometer body resulting in excellent wavelength assignment and throughput stability. The spectrometers exhibit a precision of 0.1-0.2% under constant temperature conditions.

Table 1. Instrument characterization.

Wavelength range:	280-680 nm
Wavelength resolution:	~1.8 nm FWHM at 297 nm
Calibration lamp uncertainty:	5% in UV-B and 3% in UV-A and visible
Detection limit:	0.1 W/m2
Precision:	0.1-0.2 % depending on wavelength
Data Rate:	0.1 to 1 Hz
Weight:	<23 kg per instrument
Power:	<15 amps of 28 volt DC per instrument
Location on WB57F:	Radiation boat and lower transition region

In NCAR/ARIM laboratory the wavelength dependent band pass and wavelength accuracy of the CAFS instrument was verified using a standard Hg lamp. The singlet Hg lines were measured at 296.728, 302.150, 334.148, 404.656, 435.84, and 546.07 nm wavelengths [10] by the CAFS instrument to determine the wavelength dependent band passes. The fullwidth at half intensity maximum was determined from the measurements at the six Hg lines and is shown in Figure 2a.

The manufacturer provides a function for the wavelength calibration for the spectrometer that was fitted at specific Hg and Ar lines. The wavelength calibration of the CCD spectrometer was verified in the laboratory by measuring known emission singlet lines from the Mercury lamp at six wavelengths. The centroids were calculated from the measurements of the Hg lines, and were compared to the literature values. Figure 2b presents offsets of the centroids measured with the CFAS instruments at several wavelengths from the literature values of the Hg lines under normal conditions (20-degrees C temperature and 1 atm pressure). This data is used in later sections of the paper to apply a fitted Gaussian function to the modeled data.

The calibration of the instrument is performed prior to the flight under field conditions. The stabilization of the instrument in flight to 1 atm pressure and surface temperature is

attempted in each flight. Pressure stabilization is achieved by keeping the CCD array pressurized on board the aircraft. The CCD temperature is controlled in flight by heaters. Nevertheless, all in-flight temperature and pressure offsets are recorded by the computer during the operation and are available for assessment of the data quality after the flight. The laboratory studies of the spectral shifts in the CCD array in response to the temperature and pressure variability will be discussed in a separate paper (Hall et al, paper in preparation).

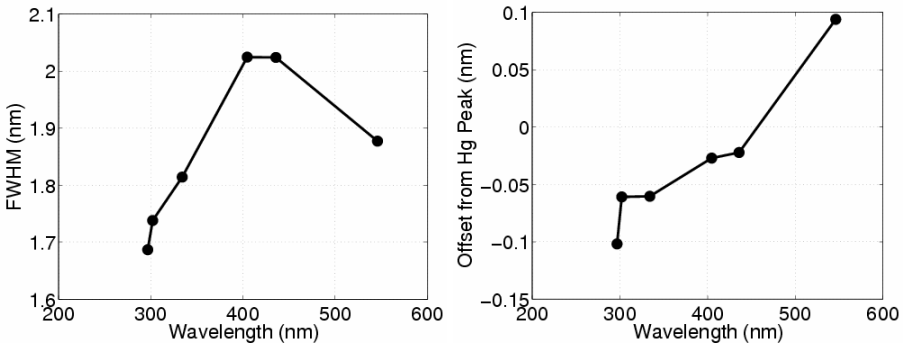

Fig. 2. a) Full width at half intensity maximum measured for several of the CAFS channels. b) Offsets to literature Hg lines from several of the CAFS channels measured with standard lamps.

The accuracy of the measurements depends on the stability of the wavelength registration and knowledge of the band-pass for the specified spectral channel of the instrument. This information is deduced prior to the flight through standard lamp calibration procedures. However, the changes in the instrumental environment during the flight can also affect these parameters. Therefore, all potential wavelength shift and band-pass widening events are routinely assessed in the post-flight calibration procedures. Furthermore, prior to the ozone retrieval, the algorithm adjusts the band-pass function based on the results of the post-flight calibration test.

The effect of the 0.2 nm spectral shift on the measurement was tested in the TUV model. The shift of the band-pass centered at 310 nm alters CAFS simulated measurement by approximately 4 % at high sun elevation and as much as 7 % at low sun elevation. The change in actinic flux decreases at longer wavelengths, while the smallest effect is found at wavelengths outside of ozone absorption bands. In addition to the spectral shifts, the change of the band-width of the CAFS channels can be caused by the temperature instability of the instrument. We tested the effect by changing the band-pass width by 13 %. However, the effect on the individual wavelengths was estimated to be less than 2 % and did not have significant dependence on SZA or altitude of the aircraft. We will discuss the effect of the spectral shift and band-pass broadening on the ozone retrieval in sections 4.1 and 6.1.

The effect of random measurement precision on the CAFS retrieved ozone was studied by adding 0.5 % random noise to the synthetic data prior to the retrieval. The changes to the measurements were estimated at one standard deviation level. The results of the measurement uncertainty on the retrieval will be discussed in the following sections.

3 RETRIEVAL ALGORITHM

The algorithm derives ozone column above the aircraft. Several auxiliary parameters are used in the retrieval such as altitude of the aircraft, solar zenith angle and surface reflectivity. The solar zenith angle is calculated at the ground level based on the aircraft geo location (latitude

and longitude), Julian date and universal time of the measurement [11]. Surface reflectivity is derived from actinic flux measurement at 360 nm and assumed to be wavelength independent.

The partial ozone column retrieval algorithm relies on look-up tables of actinic flux. The look-up table parameters and their ranges are summarized in Table 2. Actinic flux data is spectrally resolved at 0.05 nm steps, and a function of ozone, altitude, solar zenith angle, and surface albedo. The look-up tables were created using TUV V4.2 radiative transfer (RT) code [12]. Bass and Paur set of ozone absorption coefficients [14] and SUSIM/Atlas-3 solar flux measurements [15] were used for simulations of look-up tables. The TUV calculations were represented in the atmosphere by a single set of temperature, pressure and altitude profiles [16]. The ozone profiles used for simulations were derived from the latitude-dependent climatology and are total ozone (TO) dependent where TO ranges from 125 to 575 DU [17]. No aerosols and clouds were used in the look-up table simulations.

Table 2. Look-up table parameters and their range

Parameter	Range	Grid resolution
Wavelength:	305-385 nm	0.05 nm
Ozone profiles :	Low latitudes: 225 - 325 DU Middle Latitudes: 225 - 575 DU High Latitudes: 125 - 575 DU	50 DU 50 DU 50 DU
Altitude:	0 – 22 km	1 km
Solar zenith angle:	10-70 degrees, 70-86 degrees,	5-degrees 2-degrees
Surface albedo:	0.03, 0.10, 0.70	variable

Before the look-up tables can be used for comparisons with CAFS measurements the convolution of the spectrally resolved actinic flux over the band-pass is done for selected spectral channels of the CAFS instrument. The wavelengths given in the look-up tables were calculated in a vacuum, whereas the spectral calibration of the instrument was done at the Earth surface under standard pressure and temperature. During the flight CAFS' pressure and temperature were stabilized to the surface temperature and pressure. Therefore, prior to spectral convolution of the actinic flux in the look-up tables with the band-pass functions, the wavelength registration of the CAFS band-passes is adjusted to the spectral shift caused by refraction in the air corresponding to the stabilized instrumental pressure and temperature [18]. Additional wavelength adjustments to the band-pass functions are done if post-flight analyses of the CAFS spectral data suggest any wavelength shifts with respect to the Fraunhofer Solar lines [19].

Interpolation between the actinic flux in the look-up tables was done linearly to adjust for the aircraft altitude and SZA at the time of CAFS observations. The uncertainties in ozone retrieval due to linear interpolation will be discussed in subsection 4.2.1. The surface albedo was chosen arbitrarily at 3 % for all retrieved data [20][21]. The uncertainties in retrieval due to albedo assumptions will be address in subsection 4.2.3. The retrieval scheme uses CAFS measurements at several spectral channels centered at 310, 320, 330, 340 and 350 nm. The spectral triplets are formed (310/320/330, 320/330/340, and 330/340/350 nm) prior to retrievals to minimize any atmospheric interference that has linear spectral signature (such as surface albedo, some aerosols and clouds). The method of combining measurements at several wavelengths that are equally distant from each other is traditionally used in the Dobson total ozone retrieval method [6]. A combination of solar measurements taken at two wavelengths can be used to retrieve ozone after the Rayleigh scattering contribution is accounted for. However, in the presence of additional atmospheric attenuators (such as particulates or

aerosols), two wavelength pairs would have to be used. The method works under condition that the spectral attenuation from particulates should be the same in both sets of wavelength pairs. Therefore, it would cancel out after two sets of measurements were combined. The uncertainties in the retrieved ozone column associated with this assumption are discussed in section 4.2.

The first triplet is used for SZA less than 70-degrees; the second triplet is used for retrievals at SZAs larger than 70 degrees, and the third triplet is reserved for measurements at SZAs larger than 82 degrees. The sensitivity of the instrument to the light at shorter wavelengths is limited to approximately 86-degrees SZA. Therefore, the retrieval is restricted to the SZA less than 86 degrees.

4 Retrieval Uncertainties

The uncertainties in the retrieved ozone due to measurement uncertainties are discussed in section 4.1. Among tested parameters are the random measurement noise, potential spectral shifts and band-pass changes in the CAFS measurements. The retrieval uncertainties due to atmospheric parameters that are not included in the look-up tables are addressed in section 4.2. Several tests are performed to assess sensitivity of the ozone retrieval to the altitude and SZA interpolation, ozone profile variability, surface albedo uncertainties, temperature profile uncertainties, and effects of underlying clouds and aerosols. The look-up tables for 275 DU standard ozone profile and 3 % surface albedo are chosen for sensitivity tests. The CAFS spectral band-pass is modeled by a normalized Gaussian function based on the NCAR/ARIM laboratory information of the band's shape. The convolution of the band-pass function with spectrally resolved actinic flux is done either based on the look-up tables or by using special actinic flux simulations where additional atmospheric parameters are included. The retrieval is applied to the two sets of simulations, and changes in the ozone retrievals are summarized in Table 3. The range of results at different altitudes and solar zenith angles is included in the table to address the variability in the algorithm performance under typical observing conditions.

4.1 Measurement uncertainties

First, we tested the effect of the random measurement noise on the retrieval. We added 0.2 % random noise to synthetic CAFS data and estimated differences in the retrieved ozone over the typical flight altitude range (between 12 and 18 km) and over the nominal range of SZAs (between 20 and 70 degrees). We found that the change in the retrieved ozone caused by the measurement noise was less than 1.5 percent at 35-degrees SZA and 18 km altitude. In addition, the sensitivity of results to the altitude of the measurement was insignificant. Still, the effect of the measurement noise on the ozone retrieval was amplified to about 2 % change at 20-degrees SZA, while it was reduced to about 1 % at 70-degrees SZA. Moreover, the CAFS measurements were systematically averaged over 6-seconds time period in each AVE mission, which reduced random measurement noise in the CAFS data and minimized ozone retrieval uncertainty to less than 1 %.

Potential spectral shifts in the CAFS measurements can contribute to uncertainties of theretrieved ozone. In order to simulate the effect of the band-pass shift on the CAFS measurements the band-pass function was shifted by 0.2 nm to the longer wavelengths. (The choice of the 0.2 nm wavelength shift is somewhat arbitrary based on results of the pre-flight calibrations of the CAFS instrument performed at the ground level. A more accurate summary of the spectral shift in the CAFS in-flight data will be addressed in the paper (S. Halls et al., in preparation). Uncertainties in retrieved ozone due to the tested 0.2 nm band-pass shift revealed some SZA dependence, and were found to be as large as 10 % at high sun elevations, and as small as 3 % under low sun conditions. The altitude effect on uncertainties was found

to be insignificant. A discussion regarding changes in the retrieved ozone column due to spectral shifts is given in Section 6.

The temperature changes experienced by the instrument under extreme in-flight conditions could result in the broadening of the band-pass. The sensitivity of the retrieved ozone to the changes in the band-pass was studied. The CAFS data were simulated by convolution of the actinic flux tables and spectral band-pass function, where band-pass' half-width was increased by 13 percent. The uncertainties in retrieved ozone were less than 1.5 % at small SZAs, whereas at large SZAs the effect of the band-pass width was insignificant. Additional discussion regarding in-flight shifts detected during the CR-AVE 2006 campaign is given in Section 6.

Table 3. Systematic uncertainties in RT ozone column above the aircraft altitude due to sensitivity of CAFS measurements to atmospheric factors. Most of the results are shown for retrievals of the CAFS measurements simulated with restricted field of view. Sun elevation is set at 35-degrees SZA, and actinic flux is attenuated by 275 DU standard ozone profile at 12, 16, and 18 km altitude. Results in parenthesis in the second row show a range of uncertainties between 20 and 70-degrees SZA. The numbers in square parenthesis in the upper row show retrieval uncertainties for measurements with unrestricted filed of view.

		12 km	16 km	18 km
1	Altitude interpolation	<-0.1 % [-0.1%] (-0.08%/-0.12%)	<-0.1 % [-0.3%] (-0.02%/-0.06%)	~0 % [-0.2%] (-0%/-0.08%)
2	SZA interpolation	0.10% [0.1%] (-0.4%/-0.0%)	0.15% [-0.2%] (-0.7%/-0.1%)	0.20% [-0.1%] (-1.1%/+0.5%)
3	Ozone profile	0.2% [0.4%] (0.3%/0.1%)	0.75% [1.0%] (0.8%/0.3%)	0.9% [1.4%] (1.0%/0.4%)
4	Surface albedo (20 SZA/70 SZA)	3 % [3.5 %] (4.5 % / 0.8 %)	1.9% [2.7 %] (3.0 % / 0.0 %)	1.6% [2.0 %] (2.3% / 0.0%)
5	Temperature profile	0.0% [1.0%]	-1.0 % [-0.3%]	-1.7% [-1.3%]
6	Clouds 4-6 km, 30 OD (20 SZA/70 SZA)	3.3 % [4.5%] (4.4% / 0.8%)	2.6% [3.5%] (3.8% / 0.4%)	2.4 % [3.0 %] (3.2% / 0.2 %)
7	Clouds 10-12 km, 30 OD (20 SZA/70 SZA)	1.8 % [2.1%] (2.2% / 0.2 %)	2.1% [2.8 %] (2.9 % / 0.3 %)	2.0% [2.6 %] (2.9 % / 0.3 %)
8	Scat. Aerosols (0.3 OD)	0.9% (1.0% / 0.1%)	0.8% (0.9% / 0.1%)	0.7% (0.8% / 0.1%)
9	Abs. Aerosols (3.0 OD)	2.5% (2.6% / 0%)	2.6% (2.9% / 0%)	2.7% (3.0% / 0.1%)
10	Ozone cross-sections	-0.4 % [-0.3%]	-0.4 % [-0.1%]	-0.4 % [-0.1%]
11	Sum of rows 1,2,3,5,6,10	3.3% [4.6 %] (4.5% / 0.9%)	2.9% [3.7%] (4.1% / 1.2%)	3.1% [3.6%] (4.0% / 1.8%)
12	Sum of rows 1,2,3,5,10	0.5% [1.1%] (0.6% / 0.4%)	1.3% [1.1%] (1.5% / 1.1%)	2.0% [1.9%] (2.3% / 1.8 %)

4.2 Model uncertainties

This section addresses sensitivity of the retrievals to the atmospheric variability that is not captured in the look-up tables. The look-up tables are based on several atmospheric parameters that possess day-to-day variability, which also depend on season, latitude and altitude of the measurement. Among them are ozone profile, temperature profile, surface reflectivity, underlying clouds and aerosols.

Table 3 summarizes results of a sensitivity study, where results for each parameter are given in individual rows. Some results in the sensitivity studies showed altitude dependence. Therefore, all results are separated into three columns representing changes in the retrieval at 12, 16 and 18 km altitude levels that are representative of typical altitude range of the NASA WB-57 and DC8 operational flights during validation campaigns. The top row in each cell shows results estimated for CAFS simulations with a restricted field of view at 35-degrees SZA. Results for simulations with a full field of view at 35-degrees SZA are shown in square brackets. At each altitude and each parameter, a sensitivity study was carried out over a range of SZAs. The second row in each cell represents changes in retrieved ozone at 20 and 70-degrees SZA (data is shown in the parenthesis and separated by the slash sign), where restricted field of view of the instrument was applied in CAFS measurement simulations.

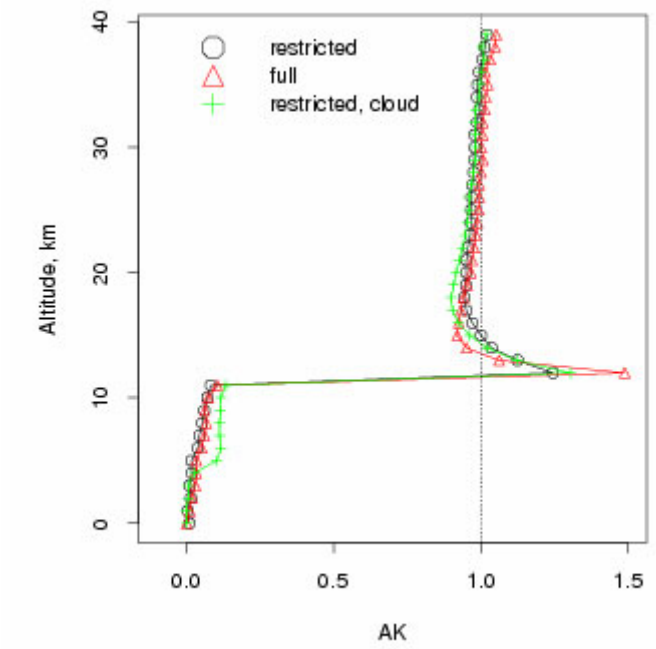

Fig. 3. CAFS sensitivity to ozone variability as function of altitude. Results are shown for measurements at 12 km altitude at 25-degrees solar zenith angle. The curves are shown before ("full", red triangles) and after ("restricted", black circles) horizon view was blocked. An example of the AK with restricted field of view and altered by the underlying cloud (30 optical depth, homogeneous layer between 4 and 6 km) is also included ("restricted, cloud", green pluses)

The Averaging Kernel (AK) method allows estimation of uncertainties in ozone column retrieval due to the shape of ozone profile [22] . The AKs are computed as a change in the total ozone (TO) column with respect to layer ozone (X) variability. This is done by normalizing a partial derivative of an actinic flux triplet (N) with respect to a layer ozone, or

$\partial N/\partial X$, to a partial derivative calculated with respect to a total ozone, or $\partial N/\partial TO$, where N is 100 x $\log_{10}$(actinic flux triplet). The AK ($\partial TO/\partial X$) is a function of altitude, solar zenith angle, and wavelength. Figure 3 shows normalized AK for the CAFS' down-welling actinic flux triple pair (310/320/330 nm) for measurements at 12 km altitude at 25-degrees solar zenith angle. The ideal AK would have no (zero) sensitivity below altitude of the measurements and full sensitivity (one) above. Since the CAFS' AK is not ideal, it will possess some sensitivity to ozone vertical distribution. Figure 3 shows that the source of the ozone retrieval error is caused by the imperfect AK profile that is greater than 1 between 12 and 20 km and less than 1 above 35 km. The profile shape difference above 35 km altitude would produce small errors in partial ozone column retrievals because of low ozone concentrations in the upper atmosphere. Another source of the retrieval error is the sensitivity that is greater (smaller) than 1 near the aircraft altitude (directly above it). Since the function is highly peaked, the amount of ozone inside the function is quite small, so the error resulting from it would be small. It would also partially compensate an algorithm's reduced sensitivity to ozone above the peak.

Prior to the June 2005 AVE campaign the CAFS design was modified to reduce its sensitivity to variability of scattered light over an inhomogeneous background. Figure 3 demonstrates normalized AKs before (full) and after (restricted) optical adjustment in the CAFS design. The "restricted" design (black open circles) reduces instrument sensitivity to atmospheric variability in the 1-km layer above the altitude of the measurement (at 12 km) as compared to the "full" design (red triangles). Both examples are given for actinic fluxes modeled without cloud or aerosol interference. However, in the presence of underlying clouds (Figure 3, green plus symbols), the AK shows an increased sensitivity above the bright surface of the cloud as well as small changes to the sensitivity above the aircraft level. The cloud in this case is simulated as a 2-km thick, 30 optical depth, horizontally infinitive, homogeneous layer of water droplets, based at 4 km altitude. Further discussion about effects of clouds on ozone retrieval can be found in sections 4.2.5 and 6.3.

4.2.1 Altitude and SZA interpolation.

A sensitivity of the ozone retrieval to interpolation errors is described in this section. The retrieval algorithm linearly interpolates the look up tables to the altitude and SZA of the measurement. The altitude interpolation is done between actinic fluxes chosen at two adjoining altitude levels that are set at 1 km apart in look up table grid (see Table 2). The changes in the retrieved ozone due to altitude interpolation are found to be less than 1 % over the range of tested altitudes and solar zenith angles (see Table 3, row 1). Sensitivity of the algorithm retrieval is tested for the assumption of linear changes in actinic flux between nominal SZAs (see Table 2 for SZA grid). The results are summarized in Table 3, second row. It was found that at higher altitudes (18 km) and small solar zenith angles, (20 degrees) the interpolation error could cause a 1 % underestimation in the retrieved ozone. However, at lower altitudes and larger SZAs the effect is significantly reduced.

4.2.2 Profile shape

Sensitivity of the ozone retrieval to the profile shape was tested by using a sub-set of the MLS-derived [23] ozone profiles selected between 22 and 44 degrees at Northern latitudes during June 2005. The mid-latitude ozone profiles from the updated TOMS climatology (see above) were chosen for look-up tables. The changes in the retrieved ozone column were calculated using AK method (see discussion above) applied to the differences between the MLS and climatological ozone profile (STD), which initially were interpolated to the MLS total ozone column. Profile residuals were integrated above the aircraft level using AK*(MLS-STD) method, while below the aircraft level (1-AK)*(MLS-STD) equation was used instead. Finally, the two, above and below, results were combined for an estimate of the

profile effect on the ozone column retrieval. Estimated sensitivity of the retrieved partial ozone column to the profile shape was found to be less than 1 % at 18 km altitude and 35-degrees SZA. Results varied very little at high sun, whereas at SZAs above 40-degrees the profile sensitivity gradually dropped to less than 0.4% at 70–degrees SZA. In addition, the sensitivity to ozone profile at 16 km altitudes was less than at 18 km, whereas at 12 km it became insignificant (see Table 3, third row for more details). At the same time, differences between analyzed the sub-set of MLS and standard middle latitude ozone profiles were also found to change with altitude. The ozone in MLS profiles was typically as much as 5 DU higher at 35 km and 3 DU lower at 25 km than the standard profile, while the difference near the surface and at 30 km altitude was minimal. Since the shape of the AK suggests that the strongest sensitivity of the retrieval to ozone profile is found within few km above the altitude of the observation, ozone variability within that altitude range would contribute the most to the retrieved ozone column uncertainty. Therefore, 2 DU ozone difference at 18 km altitude (as compared to 1 DU at 12 km) contributed to larger retrieved uncertainties in ozone column above 18 km, as compared to ozone column retrieved above 12 km, which explains altitude dependent results in the Table 3.

4.2.3 Underlying surface reflectivity

A response of the ozone retrieval to the choice of underlying reflectivity is assessed in this section. Synthetic CAFS data was simulated in the TUV code by setting surface UV reflectivity at 70 % (such as snow or clouds). The look-up tables were based on 3 % surface reflectivity conditions. The same reference ozone profiles were used in simulations with 70 and 3 % reflectivity conditions. The difference between retrieved and reference ozone columns at several altitudes are shown in Table 3 (row 4). Simulations suggest that sensitivity of the retrieval to the surface reflectivity increases at lower altitudes (up to 3 %) and can be as high as 5 % at high solar elevations (see Table 3). In cases of the measurements with full field of view sensitivity test suggests that the expected change in retrieved ozone column can be even larger by an additional 0.5 % (uncertainties are minimized by triplets as discussed above).

The underlying albedo change can produce two types of errors in ozone retrieval based on measurements of the radiances attenuated in the UV Solar spectrum. One source is related to a non-linear change in the measured N-values in response to the albedo change. It typically causes an underestimation in the ozone column retrieval. However, the ozone retrieval becomes less sensitive to the albedo change at the shorter UV wavelengths where the ozone sensitivity is the strongest. Therefore, this error would be reduced whenever the first triplet is used in the retrieval (most of the time). Another source of the retrieval error is related to the enhancement in the air-mass factor due to increased surface reflectivity. Since the photon path through the ozone layer is increased by the multiple scattering effects, its attenuation prior to the observation becomes stronger as compared to the direct sun light attenuation. However, this second type of error is also relatively small. It is minimized at higher altitudes where multiple scattering is reduced, whereas at lower altitudes the ozone amount below the aircraft is small, which also reduces the error. In addition, at large SZAs the sensitivity to the underlying surface is also strongly reduced due to reduced amount of photons reaching the surface. This second type of error typically results in the overestimation of the retrieved ozone column.

4.2.4 Atmospheric temperature

This section describes a sensitivity of the CAFS ozone retrieval to variability of atmospheric temperature. CAFS data was simulated with a January climatological temperature profile typical for tropical latitudes [24], whereas the reference (look-up) tables were based on the 1976 Standard US Atmosphere profiles for middle latitudes [16]. Both simulations were set to

the same reference ozone profiles (the mid-latitude TOMS climatology [17]) and 3 % surface reflectivity. The temperature associated change in retrieved ozone column was found to be less than 1 % at 12 km altitude. However, the effect was amplified at higher altitudes in concurrence with the differences between the two selected temperature profiles (see Table 3, row 5). No significant SZA dependence was found in the results of the temperature test.

4.2.5 High- and low-altitude clouds

The effect of the underlying clouds on the retrieved ozone is similar to the effect of the increased surface albedo (see more discussion in section 4.2.3). An effect of cloud interference in the ozone retrieval was tested by simulating actinic flux over a horizontally homogenized cloud layer. Cloud optical parameters are selected to represent a typical water cloud with log-normal size distribution of particles, effective radius of ~8 μm, and ~0.2 g/m^3 in liquid water content (clean stratus from Table 1 in [25]). A spectrally independent optical depth of 30 is chosen to optically define the continental stratiform cloud layer. A single scattering albedo of 0.9999 and an asymmetry factor of 0.85 are chosen to define scattering parameters of the cloud [26][27]. The cloud phase function is approximated by Henyey-Greenstein model [28][29]. An example of the AK with cloud interference (green pluses) is shown in Figure 3 for CAFS observations at 12 km altitude.

Sensitivity of the ozone retrieval to the vertical position of a cloud was tested by placing a 2-km thick, horizontally infinitive, homogeneous cloud layer at either 4 or 10 km altitude. Changes in the retrieved ozone column instigated by cloud scattering interference in the CAFS measurements were estimated at several altitude levels. Results are summarized in Table 3: the 6th row presents results for a tropospheric cloud located between 4 and 6 km altitude, and the 7th row shows results for a low-stratosphere altitude cloud located between 10 and 12 km altitude. It is found that the cloud layer affected retrievals at all levels, while the effect is stronger in the case of the low-altitude cloud, as well as at the lowest tested altitude of 12 km (~3.3 %). Results also indicate strong SZA dependence, where the largest change of 4.5 % is found in the retrieved ozone column at 20-degrees SZA and altitude of 12 km. The errors are smaller when the cloud is placed at a higher altitude of 10 km. However, effect of clouds on the retrieval is practically non-existent at large SZAs.

A cloud screening can be performed by using an effective albedo derived from the CAFS measurements at 360 nm wavelength channel (see the discussion in section 6.3). However, it is not done in the version of the algorithm described in this paper.

4.2.6 Absorbing and non-absorbing particulates

The effect of aerosol interference in the ozone retrieval was tested by simulating actinic flux in an aerosol-loaded atmosphere. The non-absorbing aerosols were defined by optical depth of 0.3, single scattering albedo of 1, and asymmetry factor of 0.6. Single scattering albedo of 0.9 and optical depth of 0.3 were chosen to define absorbing aerosols [30]. The effect of both scattering (Table 3, row 8) and absorbing aerosols (not shown in the table) was less than 1 % in retrieved ozone changes. However, simulations with 10-fold larger aerosol optical depth (biomass burning smoke measurements during SCAR-B campaign in 1995 [31]) for absorbing aerosol created changes in retrieved ozone (as large as 3 %) comparable to the effects of the low-altitude clouds (3.3 % for a cloud at 4-6 km) whereas cloud optical depth was ten-fold larger than the aerosol optical depth (see Table 3, compare rows 6 and 9). The altitude effect on the aerosol sensitivity test was small, while the effect was significantly reduced at larger SZAs (0.1 %).

4.2.7 Spectroscopic datasets

Results of ozone column retrievals are closely related to the a priori knowledge of absorption properties of the atmosphere. Multiple parameterizations of ozone absorption cross-sections and their temperature dependences are available from multiple sources [32]. A comparison between these datasets has been discussed in multiple scientific publications and with respect to their effects on ozone retrievals in various satellite retrieval applications [33]. The actinic flux look-up tables for CAFS ozone retrievals are based on widely used work by Bass and Paur [14]. Table 3 (10th row) contains results of the test performed on the sensitivity of the retrieval to the choice of spectroscopic datasets. Several sets of synthetic actinic fluxes were simulated using alternative sets of ozone cross-sections. The ozone retrievals were performed using the described above set of look-up tables. Simulations based on an alternative dataset described in published works by Malicet et al. [34] and Brion et al. [35] created small (0.4 %) reduction in retrieved ozone, with practically no altitude or SZA dependence (results are summarized in Table 3, row 10). Similar results were achieved for simulations that used the Bass and Paur modified cross-section dataset [36]. Among all tested spectroscopic datasets, the dataset from published work by Molina and Molina [37] produced the largest changes in retrieved ozone column, with maximum of 1.6 % (or 1.3 % for a full field of view configuration) reduction in ozone column retrieved above 18 km altitude under 20-degrees SZA conditions (results are not included in Table 3).

4.2.8 Combined geophysical uncertainties

The retrieval approach of combining measurements at three equal-distant wavelengths allows for minimization of spectral interferences that are linear in the spectrum. The above described sensitivity studies showed that the largest uncertainties in the ozone column retrieval can be related to the presence of underlying clouds. The changes in retrieved ozone were increased at high sun conditions and lower altitudes. The underlying surface albedo was the next largest parameter causing uncertainties in the retrieval, while absorbing aerosols produced comparable effects. Nevertheless, these errors can be corrected to some degree in the retrieval code based on information from "effective" reflectivity derived from the CAFS measurements at 360 nm channel (see more details in Section 6.3). More work is required for a full assessment of the retrieval accuracy after application of the reflectivity correction. Furthermore, in-flight uncertainties of other geophysical parameters important for retrieval, such as temperature and ozone vertical distribution, as well as absorption and scattering cross-section datasets, will continue to contribute to the uncertainties of the retrieval.

5 SOFT CALIBRATION AND VALIDATION AGAINST OTHER OZONE COLUMN MEASUREMENTS

The so-called "soft calibration" procedure helps to minimize uncertainties in the retrieval due to CAFS calibration uncertainties or in-flight instability in the measurements. In Sections 2 and 4.2.7 we discussed effects of spectroscopic uncertainties on ozone retrieval. Moreover, CAFS measurements are not calibrated against extraterrestrial flux. Therefore, a spectral bias between the observations and the look-up tables has to be removed prior to processing of the CAFS data.

For example, the structure in the actinic flux seen by the CAFS up-looking instrument on the test flight on January 20, 2005 was compared against the extra-terrestrial solar (ETS) flux. We used high resolution ETS flux data measured by the SUSIM instrument on the ATLAS-3 space shuttle mission [15][38] for convolution with the CAFS band-pass function (see section 2.4). A straight line was fitted to both the SUSIM data as well to the CAFS data to remove linearly varying (with wavelength) components, including Rayleigh and Mie scattering. Figure 4 shows spectral differences between the CAFS and SUSIM data.

Since the atmospheric absorption in the 340-400 nm atmospheric window is very weak, less than 0.5%, and the Ring Effect caused by the Raman scattering is also less that 0.5% for a 1.8 nm band-pass instrument, CAFS residuals are expected to show the Fraunhofer line structure convoluted with the band-pass of the instrument at the 1% level. However, the difference between the two sets was found at the ± 3-5% level. Changing the assumed FWHM from 1.8 to 1.6 nm did not change the results significantly. Therefore, the unexplained residuals between the look-up tables and the CAFS data have to be corrected.

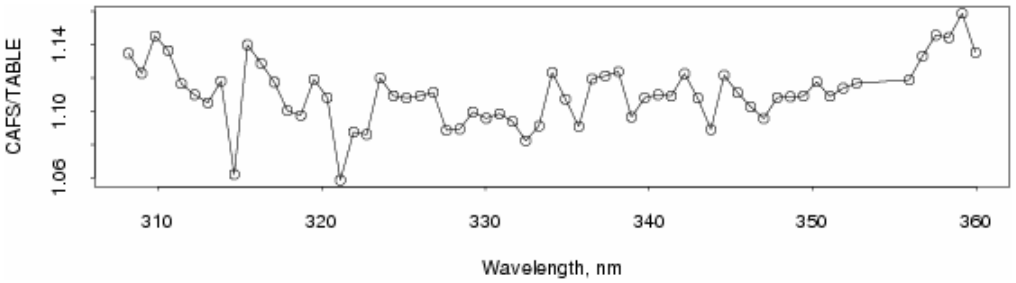

Fig. 4. "Soft calibration" parameters for zenith (DN) actinic fluxes measured by CAFS on January 20, 2005.

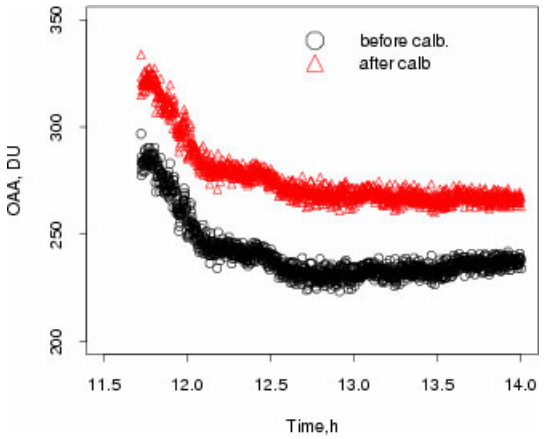

Fig. 5. Changes in the CAFS retrieved OAA during January 20, 2005 flight. Black symbols show preliminary OAA data derived from the original CAFS measurements (marked as "before calb"), red symbols show final OAA data obtained after soft calibration procedure was applied (marked as "after calb").

This approach works well in defining corrections for spectral channels above 340 nm. For channels below 340 nm, the ground-based or satellite total ozone (TO) data and ozone-sonde profiles integrated below aircraft level are used to obtain reference for the ozone column integrated above the aircraft level. For example, the Ozone Monitoring Instrument (OMI) [39] was co-located with CAFS flight on January 20, 2005. At a flight time of 20:35:00 UT, for a clear sky scene (reflectivity at 360 nm is zero), TO from a co-incident OMI measurement was estimated at 310 DU. The reference actinic flux from the look-up tables is interpolated to the satellite TO, SZA and altitude of the aircraft data averaged over 1 minute time period between 20:34:30 and 20:35:30 (about 10 measurements, 51 degrees SZA, and ~11 km altitude). The measured CAFS actinic flux data were averaged over the chosen flight period for each spectral channel. Then, the ratio between reference model and CAFS data was used to minimize uncertainties in the retrieval process for all consecutive flights during the P-AVE

2005 campaign. The ratio between CAFS averaged data and synthetic data is shown in Figure 4 for down-welling CAFS data. Figure 5 shows results for time-series of ozone above the aircraft (OAA) derived from measured and corrected data taken on the January 20, 2005 flight.

The same type of spectral structure as shown in Figure 4 was found in the actinic flux observed by the CAFS up-looking instrument during the test flight on January 14, 2005. Comparisons of ~1000 spectra taken during this flight were analyzed. During the flight the aircraft pressure altitude changed from 950 hPa to 200 hPA and solar zenith angle changed from 71 to 85 degree, yet all 1000 spectra fell so closely together that the line width was only slightly broadened.

Results of the tests as described above suggest that the "soft calibration" method assures good relative accuracy of ozone retrievals during a flight, as well as from flight to flight. Since the absolute accuracy of the satellite total ozone retrievals can be established in other ways – by comparison against numerous total ozone data available from the ground-based Dobson and Brewer networks – it allows for using CAFS ozone retrievals for validation of the spatial and temporal variability observed in satellite derived stratospheric ozone columns. Moreover, tracking changes in the correction factor during the flights as well as between the flights provides an excellent method for a quality control of the CAFS data. However, the correction factor has to be redefined every time when optical or technical modifications are made to the instrument. In addition, all spectral shift corrections (discussed in the following section) detected during an instrument calibration or in-flight analysis have to be applied prior to performing a "soft calibration" procedure.

6 DATA ANALYSIS

A case study of uncertainties in the ozone partial columns derived from the CAFS flight data is discussed in this section. CAFS measurements were taken aboard the NASA WB-57 during the AVE campaign in Costa Rica in the winter of 2006. The sensitivity of the retrieved ozone to spectral shifts is discussed in section 6.1. The validation of the CAFS measurements against other coincident ozone measurements is discussed in section 6.2.

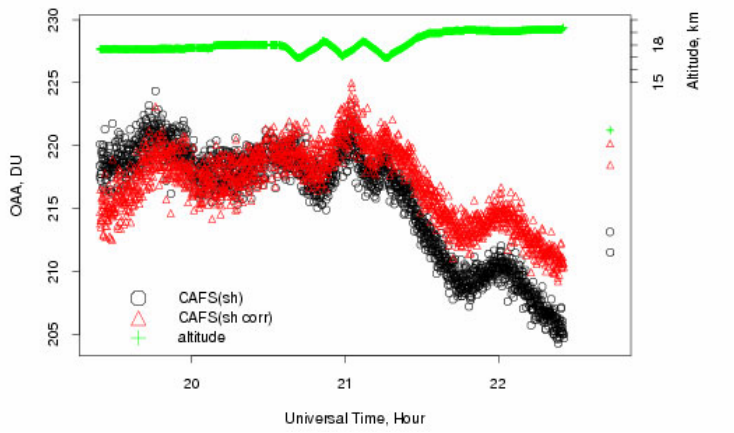

Fig. 6. The flight series of the CAFS retrieved ozone columns above the altitude of the WB-57 aircraft (green line) taken on January 25, 2006. The data before correction (black) and after correction (red) are plotted as function of time.

6.1 Spectral shifts in data

The sensitivity of the retrieved ozone to wavelength registration shifts was discussed in section 4.1. Here we present analysis of actual shifts detected during 2006 flights. The CAFS retrieved ozone column data were re-processed to adjust for small spectral shits due to the temperature instability of the instruments. The shifts were detected by comparing the in-flight actinic flux spectrum to the Solar Fraunhofer lines. Figure 6 shows sensitivity of the retrieved data to the shifts, where changes in retrieved ozone are altitude and time dependent (see difference between black, uncorrected and red, corrected, symbols). The reprocessed data (red triangles) show better internal consistency between the out-bound (before 20:30 UT) and in-bound (after 20:30 UT) portions of the flight that were flown in close proximity to the same rout.

6.2 CAFS retrieved ozone vs. Microtops total ozone column and ozone profile balloon measurements

During the Costa Rica AVE 2006 campaign partial ozone columns, primarily above 19 km, were derived from the CAFS observations, under a variety of sun elevations and low ozone variability over a tropical region. The CAFS ozone column retrieved data was verified during CR-AVE campaign. Co-incident and co-located data from Microtops, ozone sonde, and CAFS instruments were collected in San Jose, Costa Rica in January and February of 2006. A small subset of about 20 CAFS measurements was selected from flights at approximately 19 km altitude and in close proximity to the San Jose Airport. Launches of ozone-sondes from the University of San Jose were coincident in time with the aircraft over-pass. Multiple measurements of the total ozone column were taken by Microtops instruments at the San Jose airport over the course of the flight day. The set of 12 coincident matches was used for intercomparisons.

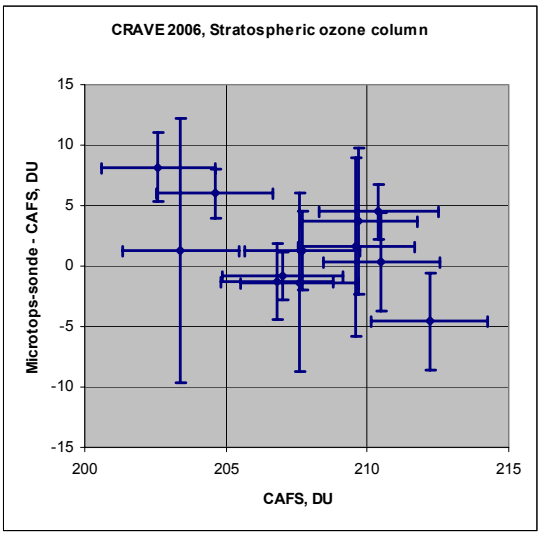

Fig. 7. Scatter plot comparisons between CAFS partial ozone above the aircraft and the residuals found between combined Microtops/sounding and CAFS data. The uncertainty bars are based on each measurements assessment of uncertainties.

For each science flight, the subset of coincident CAFS partial ozone column above 19 km was averaged over two minute time period (about 208 DU). The corresponding ozone-sonde profile was integrated below 19 km altitude and subtracted from the averaged Microtops total

column data, thus, providing an independent reference for validation of CAFS ozone column data above 19 km altitude. Figure 7 presents a summary of 12 residuals found between an independent reference and CAFS partial ozone column data during CR-AVE campaign. The residuals show a mean bias of 1 % against CAFS ozone data, while standard deviation is about 3 %. The CAFS retrieved ozone uncertainties due to spatial data averaging and ozone profile sensitivity are less then 3%. The standard deviation of daily averaged Microtops is about 3 %, but can be as high as 5%. Microtops total column and integrated ozonesonde combined uncertainties are better than 4 %. The results suggest that the CAFS partial ozone column measurements are accurate to about 3 %, whereas uncertainties in the measurements are about 5 %.

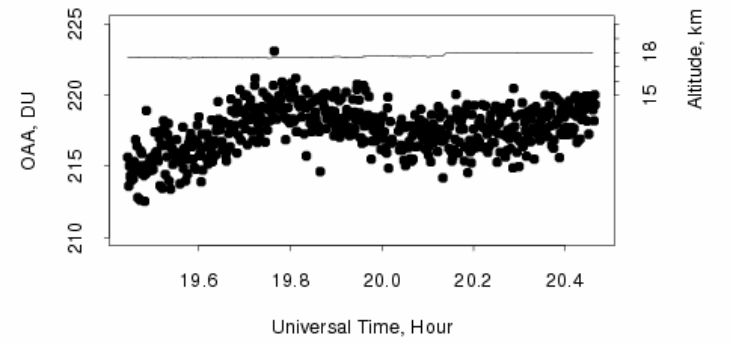

(a)

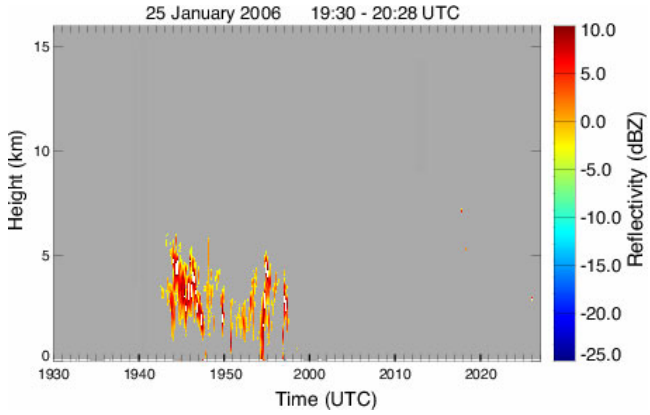

(b)

Fig. 8. a) The flight series of the CAFS retrieved ozone columns (circles) above the altitude of the WB-57 aircraft (solid line) taken on January 25, 2006 between 19:26:40 and 20:28:01 UTC. b) The time series of the approximate reflectivity derived from CRS data on board of the WB-57 over the same period of flight time.

6.3 Low-altitude cloud effect

A cloud effect was observed in the CAFS data on several occasions during the CR-AVE campaign. The effect was verified against coincident CRS (Cloud Radar System) measurements of the underlying reflectivity. Figure 8 illustrates one of the effects observed during January 25, 2006 flight. Between approximately 19:26:40 and 20:28:01 UTC, the CAFS data (circles) showed a relative increase (about 2%) in retrieved ozone while the altitude of the aircraft remained unchanged (at about 18 km, solid line in Figure 8a). At the same time coincident CRS measurements (Figure 8b) indicated the presence of the cloud. The

theoretical assessment of the effects of the cloud (30 optical depth, located between 4 and 6 km, see Table 3) on simulated actinic flux spectrum suggests a similar level of sensitivity in CAFS data (averaged SZA is 34 degrees).

The future work will focus on developing methods to correct CAFS data for high reflectivity scenes, such as cloud cover or snow on the ground. The method will match actinic flux from the look up tables to the CAFS measurements over 340-380 nm spectral range. The "effective" albedo at 360 nm can be derived by the analytical derivation of the Lambertian effective reflectivity (LER) from measured actinic fluxes similar to the TOMS LER approach [9]. Then, the full spectral range of actinic fluxes in the look up tables will be adjusted to the "effective" albedo. The updated tables will then be used to adjust retrieved partial ozone column.

7 CONCLUSIONS

This research supports AURA validation activities by deploying new instrumentation for the measurements of solar radiation on the NASA WB-57 and DC-8 platforms for the determination of ozone column abundance. These new instruments are the CCD based Actinic Flux Spectroradiometers (CAFS) to determine the down and up-welling UV and visible actinic flux as a function of wavelength. An algorithm to derive partial ozone columns from CAFS data was developed in 2004 and field-tested during 2005 and 2006. An elaborate dataset of partial ozone columns has been provided for the first-round of the Aura satellite validation: OMI ozone columns and MLS integrated ozone profiles.

During the Costa Rica AVE 2006 campaign partial ozone columns, primarily above 18 km, were derived from the CAFS observations, under a variety of sun elevations and low ozone variability conditions over a tropical region. The modified CAFS optical design was implemented to reduce sensitivity to the variability of scattered light over inhomogeneous background after the June 2005 AVE campaign. It was found, that both "soft calibration" and spectral shift corrections may be needed in the data processing. Results of the CR-AVE 2006 data analyses revealed dynamical changes in spectral shifts during flights. Therefore, the "soft calibration" technique was not effective in removing these shifts. A post-flight analysis provided information for the shift estimation. Subsequently, the shift correction was successfully applied to the data re-processing.

The CAFS retrieved ozone columns were verified during CR-AVE campaign by reference to the daily ozone-profile sounding, multiple Microtops total ozone measurements, and in-situ ozone measurements on board of the WB-57 aircraft. The results suggest that the CAFS partial ozone column measurements are accurate to about 3 %, whereas uncertainties in the measurements are about 5 %. However, when measurements are taken above the underlying clouds, the CAFS retrieval algorithm seems to overestimate partial ozone column by about 2 % (solar zenith angle and altitude dependence of this uncertainty is discussed in the paper). Other possible instrumental and spectroscopic uncertainties are minimized by "soft calibration" techniques prior to the science flights.

Comparisons between OMI total ozone column and CAFS derived partial ozone column has proven to be difficult due to the lack of tropospheric ozone estimates from the WB-57 measurements. Some AVE campaigns have the ability to derive the ozone column below the aircraft level from other remote-sensing measurements, therefore allowing for successful validation of the OMI total ozone column. For example, during the PAVE 2005 mission measurements of ozone below and above the DC-8 aircraft were taken, coincident with the CAFS measurements. Still, the CAFS measurements are best used to differentiate changes in stratospheric ozone from changes in total column ozone along the satellite tracks across a variety of changing atmospheric conditions. In particular, our future work will assess changes in stratospheric ozone over high clouds as measured by the OMI and CAFS instruments in a flight over the tropical storm Arlene in June 2005. Soon to be released OMI ozone profiles

will be validated with the CAFS partial ozone column data. The CAFS data will also be used to validate partial stratospheric ozone columns derived from the MLS instrument on board the Aura satellite.

ACKNOWLEDGEMENTS.

This work was supported by the NASA Tropospheric Chemistry Program. The authors gratefully acknowledge helpful discussions with K. Chance, R .McPeters, and E. Hilserath. We would also like to emphasize the crucial contributions of the pilots and crew of both the NASA WB-57F and DC-8 aircrafts, and the support staff associated with the Aura Validation Experiment campaign that made CAFS measurements a success. The authors would like to thank V. Holger from University of Colorado, CIRES for processing ozonesonde data during the CR-AVE campaign, and to G. Labow of NASA/Goddard for providing the Microtops instrument for total ozone column measurements. Both datasets were essential in validation of the CAFS ozone retrieval product. We would like to stress our appreciation to the professors and students from the Universidad Nacional and the Univesidad de Costa Rica for their diligent work on launching balloons during school winter break. Authors would like to acknowledge the work of Lihua Li of UMBC/GEST and G. Heymsfield of GSFC for providing CRS data. Also we would like to acknowledge NASA HQ, e.g. Hal Maring of Radiation Science Program, for funding the CRS instrument and data taking.

REFERENCES

[1] M. R. Schoeberl, A.R Douglass, E. Hilsenrath, P.K. Bhartia, R. Beer, J.W. Waters, M.R. Gunson, L. Froidevaux, J.C. Gille, J.J. Barnett, P.F. Levelt, and P. DeCola, "Overview of the EOS Aura mission," *IEEE Trans. Geo. Rem. Sens.* **44**(5), 1066-1074 (2006) [doi:10.1109/TGRS.2005.861950]

[2] H. G. J. Smit, W. Straeter, B.J. Johnson, S. J. Oltmans, J. Davies, B. Hoegger R., Stubi, F. Schmidlin, J. Witte, A. Thompson, I. Boyd, and F. Poisny, "Assessment of the performance of ECC-ozonesondes under quasi-flight conditions in the environmental simulation chamber: Insights from the Juelich Ozone Sonde Intercomparison Experiment (JOSIE)," *J. Geophys.Res.*, (2007) [doi:10.1029/2006JD007308].

[3] B. J. Johnson, S. J. Oltmans, H. Vomel, H. G. J. Smit, T. Deshler, and C. Kroger, "Electrochemical concentration cell (ECC) ozonesonde pump efficiency measurements and tests on the sensitivity to ozone of buffered and unbuffered ECC sensor cathode solutions," *J. Geophys.Res.* **107**(19), 4393 (2002) [doi:10.1029/2001JD000557]

[4] T. J. Deshler, J. Messner, H. G. J. Smit, R., Stubi, G. Levrat, B.J. Johnson, S. J. Oltmans, R. Kivi, A. Thompson, J. Witte, ,J. Davies, F. J. Schmidlin, G. Brothers, and T. Sasaki., "Balloon experiment to test ECC-ozonesondes from different manufacturers, and with different cathode solution strengths: Results of the BESOS flight," *J. Geophys. Res.*, (2007) (in press)

[5] R. D. McPeters, G. J. Labow, and B. J. Johnson, "A satellite-derived ozone climatology for balloonsonde estimation of total column ozone," *J. Geophys. Res.*, **102**(D7), 8875-8885 (1997) [doi:10.1029/96JD02977].

[6] R.E. Basher, "Review of the Dobson spectrophotometer and its accuracy," *WMO Global Ozone Res. and Monitoring Rept **13**,* Geneva (1982).

[7] R.D. Hudson and W.G. Planet, "Handbook for Dobson ozone data re-evaluation," *WMO Global Ozone Res. and Monitoring Rept. **29***, WMO/TD-No. 597, Geneva (1993).

[8] P. K. Bhartia, R. D. McPeters, C.L. Mateer, L. E. Flynn, and C. Wellemeyer, "Algorithm for the estimation of vertical ozone profiles from the backscattered

ultraviolet technique," *J. Geophys. Res.,* **101**, 18,793-18,806 (1996) [doi:10.1029/96JD01165].
[9] R. D. McPeters, P.K. Bhartia, A.J. Krueger, J. R. Herman, B. Schlesinger, C.G. Wellemeyer, C. J. Seftor, G. Jaross, S.L. Taylor, T. Swissler, O. Torres, G. Labow, W. Byerly, and R.P. Cebula, "Nimbus-7 Total Ozone Mapping Spectrometer (TOMS) data products user's guide," NASA Reference Publication 1384, Washington D.C. (1996)
[10] J. Reader, and C. H. Corliss, "Wavelengths and Transition Probabilities of Atoms and Atomic Ions," *NSRDS-National Bureau of Standards* **68** (1980).
[11] J. Meeus, *Astronomical Algorithms*, Willmann-Bell, Richmond, Virginia, U.S.A., (1991).
[12] S. Madronich and S. Flocke, "The role of solar radiation in atmospheric chemistry," in *Handbook of Environmental Chemistry,* Boule Ed., 1-26, Springer_Verlag, Heidelberg (1998).
[13] B. L. Lefer, R. E. Shetter, S. R. Hall, J. H. Crawford, and J. R. Olson, "Impact of clouds and aerosols on photolysis frequencies and photochemistry during TRACE-P: 1. Analysis using radiative transfer and photochemical box models," *J. Geophys. Res.* **108**, 8821 (2003) [doi:10.1029/2002JD003171]
[14] A. M. Bass and R. J. Paur, "The ultraviolet cross-sections of ozone. I. The measurements. II.- Results and temperature dependence," in *Atmospheric ozone, Proceedings of the Quadrennial Ozone Symposium*, C.S. Zerefos and A. Ghazi Ed., 606-610, Reidel, Dordrecht, Boston, Lancaster (1985).
[15] M.E. VanHoosier, "Solar ultraviolet spectral irradiance with increased wavelength and irradiance accuracy," *SPIE Proceedings* **2831**, 57-64 (1996) [doi:10.1117/12.257210].
[16] *US Standard Atmosphere Supplements*, US Govt. Printing Office, Washington, D.C. (1976)
[17] R.D. McPeters, G. J. Labow, and J. A. Logan, "Ozone climatological profiles for satellite retrieval algorithms," *J. Geophys. Res.* **112**, D05308 (2007) [doi:10.1029/2005JD006823].
[18] D. R. Lide, *CRC Handbook of Chemistry and Physics,* Internet Version 2007, 87th Edition, Taylor and Francis, Boca Raton, FL (2007) http://www.hbcpnetbase.com.
[19] K. Chance, "Ultraviolet and visible spectroscopy and spaceborne remote sensing of the Earth's atmosphere," *C. R.. Physique* **6**, 836-847 (2005). [doi:10.1016/j.crhy.2005.07.010]
[20] M. Blumthaler, and W. Ambach, "Solar UVB-albedo of various surfaces, " *Photochem. Photobiol.* **48**, 85– 88 (1988) [doi: 10.1562/0031-8655(2001)073<0366:AEMUIM>2.0.CO;2].
[21] R. L. McKenzie, M. Kotkamp, and W. Ireland, "Upwelling UV spectral irradiances and surface albedo measurements at Lauder, New Zealand," *Geophys. Res. Lett.* **23**, 1757– 1760 (1996) [doi:10.1029/96GL01668].
[22] C. D. Rodgers, *Inverse methods for atmospheric sounding: Theory and practice*, World Science, Singapore (2000).
[23] N. J. Livesey, W. G. Read, L. Froidevaux, J. W. Waters, M. L. Santee, H. C. Pumphrey, D. L. Wu, Z. Shippony, and R. F. Jarnot, "The UARS Microwave Limb Sounder version 5 data set: Theory, characterization, and validation," *J. Geophys. Res.* **108**, 4378-4398 (2003) [doi:10.1029/2002JD002273].
[24] M. E. Summers and W. Sawchuck, "Zonally averaged trace constituent climatology. A combination of observational data sets and 1-D and 2-D chemical-dynamical model result," *Naval Research Laboratory, Technical Repor*t, NRL/MR/7641-93-7416, Washington, DC (1993).

[25] C. Erlick, J. Frederick, V. Saxena, and B. Wenny, "Atmospheric transmission in the ultraviolet and visible: Aerosols in cloudy atmospheres," J. Geophys. Res. **103**, 31,541-31,556 (1998) [doi: 10.1029/1998JD200053].
[26] A. S. Slingo, "A GCM parameterization for the shortwave radiative properties of water clouds." *J. Atmos. Sci.* **46**, 1419-1427 (1989) [doi:10.1175/1520-0469(1989)046<1419:AGPFTS>2.0.CO;2].
[27] Y. Hu, and K. Stamnes, "An accurate parameterization of the radiative properties of water clouds suitable for use in climate models," *J. Climate* **6**, 728–742 (1993) [doi:10.1175/1520-0442(1993)006<0728:AAPOTR>2.0.CO;2]
[28] L. C. Henyey and J. L. Greenstein, "Diffuse radiation in the galaxy," *Astrophys. J.* **93**, 70-83 (1941) [doi:10.1086/144246].
[29] J. Hansen and L.D. Travis, "Light scattering in planetary atmospheres," *Space Sci. Reviews* **16**, 527-610 (1974) [doi:10.1007/BF00168069].
[30] B.N. Wenny, V. K. Saxena and J. E. Frederick, "Aerosol optical depth measurements and their impact on surface levels of ultraviolet-B radiation," *J. Geophys. Res.* **106**, 17311–17319 (2001) [doi:10.1029/2001JD900185].
[31] J. F. Gleason, N. C. Hsu, and O. Torres, "Biomass burning smoke using backscattered ultraviolet radiation: SCAR-B and Brazilian smoke interannual variability," *J. Geophys. Res*. **103**, 31969-31978 (1998) [doi: 10.1029/98JD00160]
[32] H. Keller-Rudek and G. K. Moortgat, *MPI-Mainz-UV-VIS Spectral Atlas of Gaseous Molecules*, http://www.atmosphere.mpg.de/spectral-atlas-mainz.
[33] J. P. Burrows, A. Richter, A. Dehn, B. Deters, S. Himmelmann, S. Voigt, and J. Orphal, "Atmospheric remote-sensing reference data from GOME-2. Temperature-dependent absorption cross sections of O3 in the 231-794nm range," *J. of Quant. Spec. and Rad. Trans.* **61**, 509-517 (1999) [doi:10.1016/S0022-4073(98)00037-5].
[34] J. Malicet, D. Daumont, J. Charbonnier, C. Parisse, A. Chakir, and J. Brion, "Ozone UV spectroscopy. II. Absorption cross-sections and temperature dependence," *J. Atmos. Chem.*, **21**, 263-273 (1995) [doi:10.1007/BF00696758].
[35] J. Brion, A. Chakir, D. Daumont, and J. Malicet, "High-resolution laboratory absorption cross section of O3. Temperature effect," *Chem. Phys. Lett.* **213**, 610-512 (1993) [doi:10.1016/0009-2614(93)89169-I].
[36] J. Orphal and K. Chance, "Ultraviolet and visible absorption cross sections for HITRAN," *J. Quant. Spectrosc. Radiat. Transfer* **82**, 491–504 (2003) [doi:10.1016/S0022-4073(03)00173-0].
[37] L.T. Molina and M.J. Molina, "Absolute absorption cross sections of ozone in the 185-to 350nm wavelength range," *J. Geophys. Res.* **91**(D13), 14501-14508 (1986).
[38] T. N. Woods, D.K. Prinz, G.J. Rottman, J. London, P.C. Crane, R.P. Cebula, E. Hilsenrath, G.E. Brueckner, M.D. Andrews, O.R. White, M.E. VanHoosier, L.E. Floyd, L.C. Herring, B.G. Knapp, C.K. Pankratz, and P. A. Reiser, "Validation of the UARS ultraviolet irradiances: Comparison with the ATLAS 1 and 2 measurements," *J. Geophys. Res.* **101**, 9541-9569 (1996) [doi:10.1029/96JD00225].
[39] P.F. Levelt, G. H. J. van den Oord, M. R. Dobber, A. MŠlkki, H. Visser, J. Vries, P. Stammes, J. O. V. Lundell and H. Saari, "The Ozone Monitoring Instrument," *IEEE Trans. Geo. Rem. Sens.* **44**, 1093-1101 (2006) [doi:10.1109/TGRS.2006.872333]